Longitudinal conductivity of massless fermions with tilted Dirac cone in magnetic field

Igor Proskurin,[1,2,*] Masao Ogata,[1] and Yoshikazu Suzumura[3]

[1] *Department of Physics, The University of Tokyo, Bunkyo-ku, Tokyo 113-0033, Japan*
[2] *Institute of Natural Sciences, Ural Federal University, Ekaterinburg 620083, Russia*
[3] *Department of Physics, Nagoya University, Nagoya 464-8602, Japan*

(Dated: May 11, 2015)

We investigate a longitudinal conductivity of a two-dimensional relativistic electron gas with a tilted Dirac cone in magnetic field. It is demonstrated that the conductivity behaves differently in the directions parallel and perpendicular to the tilting of the cone. At high magnetic fields, the conductivity at non-zero Landau levels in the direction perpendicular to the tilting modifies non-trivially, in contrast to the parallel case. At zero temperature, the crossover of the conductivity at the Dirac point from high to low magnetic field is studied numerically. It is found that the tilting produces anisotropy of the conductivity which changes with the magnetic field which is different from the anisotropy coming from the Fermi velocity. We also discuss the conductivity at finite temperatures and finite magnetic fields which can be directly compared with the experiments in α-(BEDT-TTF)$_2$I$_3$ organic conductor. We find that the tilting does not affect so much the magnetic-field dependence of the conductivity except for the prefactor. We discuss the interpretation of recent experimental data and make some proposals to detect the effect of the tilting in future experiments.

PACS numbers: 72.10.–d,75.47.–m

I. INTRODUCTION

During the last decade, Dirac fermions have gained much attention in condensed matter physics being of a great interest from both fundamental and applied points of view.[1] The most prominent material where existence of massless Dirac particles was unambiguously shown is graphene.[2] Later Dirac electrons were theoretically predicted and experimentally observed in many other materials including surface states of two- and three-dimensional topological insulators,[3] α-(BEDT-TTF)$_2$I$_3$ organic conductor,[4–8] and $BaFe_2As_2$ iron-pnictide.[9] The presence of relativistic Dirac quasiparticles in these materials gives rise to such interesting physical phenomena as unconventional quantum Hall effect,[2] crossover from the positive to negative interlayer magnetoresistance,[10,11] and giant Nernst–Ettingshausen effect.[12–14]

Organic conductor α-(BEDT-TTF)$_2$I$_3$ is a layered material which consists of conducting layers of BEDT-TTF molecules separated by insulating layers of I_3^- anions. Under the hydrostatic pressure about 1.5 GPa, it undergoes a transition to the zero-gap state with a typical ratio of the in-plane to the interlayer conductivity $\sim 10^3$ which makes this compound a quasi-two-dimensional conductor.[15] Unusual transport properties[4] in α-(BEDT-TTF)$_2$I$_3$ were explained by finding the existence of the Dirac fermions in the analytical band structure calculation,[5] and numerical one.[6] Kobayashi *et al.*[7] showed that Dirac quasiparticles should be described by an anisotropic tilted Weyl equation. Further experimental and theoretical studies provided confirmation of the massless Dirac nature of the carriers in this compound.[10,11,15–17] In contrast with graphene, where the carrier concentration is easily tuned by applying the gate voltage, the carrier number in α-(BEDT-TTF)$_2$I$_3$ is always fixed near the charge neutrality point which makes difficult direct observation of the Landau levels. Recently, multilayer quantum Hall effect and Subnikov–de Haas oscillations were observed in this compound using the method of contact electrification from the substrate.[18]

A notable feature of the massless fermions in α-(BEDT-TTF)$_2$I$_3$ is considerable tilting of the Dirac cone in the energy-momentum space which breaks both the Lorentz invariance and the chiral symmetry. The properties of systems with a tilted Dirac spectrum and their realizations in real materials were studied by several authors.[19–23] It was found that in magnetic field the effect of tilting on the energy spectrum is similar to the effect of an electric field on relativistic Landau levels in graphene.[20,24] In the latter case, using the argument based on the Lorentz covariance of the Dirac Hamiltonian, it was shown that the electric field squeezes the separation between the Landau levels and shifts the positions of the wave functions in the real space.[24] Kawarabayashi *et al.*[21] found that even if the tilting is introduced, there exists the generalized chiral symmetry which provides existence and stability of the zero-mode which governs the transport properties near the charge neutrality point in high magnetic fields.[15,17]

A general problem of the transport of massless Dirac fermions was studied previously in different contexts. In relation to graphene, Shon and Ando[25] calculated the conductivity in the self-consistent Born approximation (SCBA), and Peres *et al.*[26] considered the effect of lattice defects and electron-electron interactions. Sharapov *et al.*[27] made a fully analytical calculation of the zero-temperature conductivity for gapped Dirac excitations in the context of d-wave superconductors, and the problem of Shubnikov–de Haas oscillations was studied in detail by Gusynin and Sharapov.[28] With respect to organic conductors, the effect of electron-electron interactions on

the in-plane conductivity was considered by Morinari and Tohyama.[29] The effect of tilting on the in-plane conductivity in zero magnetic field was studied previously by the authors.[30,31] In weak magnetic fields the effect of tilting on the Hall conductivity has been studied previously by Kobayashi *et al.*[32]

The purpose of this paper is to answer several questions. The first question is how the tilting of the Dirac cone affects the transport properties of two-dimensional Dirac fermions in magnetic field. The second question is how to provide an experimental confirmation of the tilting. According to the knowledge of the authors, at the present time, there is no experimental evidence of the Dirac cone tilting in α-(BEDT-TTF)$_2$I$_3$. In this paper, we make a proposal how it can be confirmed in future experiments by detecting the anisotropy in the conductivity. The third question is related to the scenario of the magnetotransport in α-(BEDT-TTF)$_2$I$_3$ which is motivated by recent experiments.[33,34] We note that at the present time the magneto-conductivity in α-(BEDT-TTF)$_2$I$_3$ is not completely understood. First-principles band-structure calculations show that, together with the Dirac cone, α-(BEDT-TTF)$_2$I$_3$ also has a heavy-hole band near the Fermi level[6] which might participate in the conducting properties. Based on this argument, the magneto-conductivity of α-(BEDT-TTF)$_2$I$_3$ in Ref. 33 was explained in the framework of quasi-classical two-carrier model where the first carriers are massless Dirac electrons, and the second are massive holes. However, taking into account recent experimental results[34], we propose an alternative explanation which is based only on the Dirac type of carriers. We discuss a criterion which can make a clear distinction between these two models.

The paper is organized as follows. In Sec. II, we develop the formalism. In Sec. III, we consider the effect of the Dirac cone tilting on the zero-temperature conductivity. In the limit of high magnetic fields, we study how the tilting modifies the conductivity when the chemical potential is situated at the nth Landau level. It is demonstrated that the conductivity in this case is determined by the wave function of the nth Landau level. Next, we study how the conductivity at $\mu = 0$ depends on magnetic field and impurity concentration. From the previous studies[25,27] we know that massless Dirac fermions at $\mu = 0$ possess universal conductivity which is magnetic field and impurity independent. We show that in the presence of the tilting this behavior, in general, changes, however, in one particular direction, the conductivity remains independent of impurities and magnetic field. We also explain that the tilting leads to the anisotropy in the conductivity which changes in magnetic field, which makes it different from another type of the anisotropy coming from the Fermi velocity. This fact can be useful for experimental confirmation of the tilting in the two-dimensional Dirac systems. Section IV is devoted to the conductivity at finite temperatures. First, we demonstrate that a combination of a crossover from weak to high magnetic fields, and the Zeeman splitting of $n = 0$ Landau level result in characteristic two-step decrease of the conductivity in the magnetic field detected experimentally.[33,34] Next, based on the self-consistent Born approximation (SCBA) arguments, we show that the magnetic-field dependence of the Landau level broadening produces minimum in the magneto-conductivity which may be crucial for understanding recent experiments.[34] We also find that the tilting does not affect so much the magnetic-field dependence of the conductivity except for the prefactor. Section V is reserved for the summary.

II. FORMULATION

A. Model Hamiltonian

The Hamiltonian for the two-dimensional relativistic electron gas inside the layer of BEDT-TTF molecules in magnetic field (for a given valley) can be written in the form of the generalized Weyl Hamiltonian[5,19]

$$H = v_F \left(\eta \Pi_y \sigma_0 + \Pi_x \sigma_x + \Pi_y \sigma_y \right), \tag{1}$$

where v_F is the Fermi velocity, $\Pi_i = -i\hbar\nabla_i + eA_i$ denotes a canonical momentum, σ_i is the Pauli matrix ($i = x, y$), with σ_0 being the unitary matrix, A_i is a magnetic vector potential, and $-e$ is an electron charge. Here, we consider the case of a tilted Dirac cone with the isotropic Fermi velocity due to the fact that the angular dependence of the Fermi velocity is small in α-(BEDT-TTF)$_2$I$_3$.[8] We comment on the effect of the anisotropy of the Fermi velocity at the end of Sec. III. Without loss of generality, we imply that the Dirac cone is tilted in the y-direction with $0 \leq \eta < 1$ being a degree of the tilting.

The eigenvalue problem for the Hamiltonian in Eq. (1) in the Landau gauge $\boldsymbol{A} = (0, Bx, 0)$ can be solved by algebraic methods which gives the following spectrum[11,35]

$$E_n = \operatorname{sgn}(n) \sqrt{2eB\hbar v_F^2 \lambda^3 |n|}, \tag{2}$$

and eigenfunctions

$$\Psi_{kn}(x, y) = \frac{e^{iky}}{\sqrt{\ell L}} \Phi_n \left(\frac{x - x_n + \ell^2 k}{\ell} \right), \tag{3}$$

where

$$\Phi_n(x) = \frac{\chi^{(-)} h_{|n|}(x) - i \operatorname{sgn}(n) \chi^{(+)} h_{|n|-1}(x)}{\sqrt{2(2 - \delta_{n0})(1 + \lambda)}}, \tag{4}$$

$n = 0, \pm 1, \pm 2, \ldots$, $\lambda = \sqrt{1 - \eta^2}$, $\ell = \sqrt{\hbar/eB}$ is the magnetic length, k and L are the wave number and the size of the system in the y-direction, where periodic boundary conditions are implied, $x_n = -\operatorname{sgn}(n) \eta \ell \sqrt{2|n|/\lambda}$, $\chi^{(+)} = (1 + \lambda, -i\eta)^{\mathrm{T}}$ [$\chi^{(-)} = (i\eta, 1 + \lambda)^{\mathrm{T}}$] denotes the eigenvector of a generalized chiral operator[21] $\gamma = (\sigma_z - i\eta\sigma_x)/\lambda$

corresponding to $+1$ (-1) eigenvalue,

$$h_{|n|}(x) = \frac{\lambda^{1/4}}{2^{|n|/2}\pi^{1/4}\sqrt{|n|!}} \exp\left(-\frac{\lambda}{2}x^2\right) H_{|n|}\left(\sqrt{\lambda}x\right), \tag{5}$$

and $H_n(x)$ denotes the nth Hermite polynomial; $\mathrm{sgn}(x)$ is defined as -1 for $x<0$, 0 for $x=0$, and $+1$ for $x>0$. Each Landau level is multiply degenerated with respect to k with the degeneracy factor $V/(2\pi\ell^2)$ where V is a two-dimensional area of the system.

In what follows, we consider the Hamiltonian in Eq. (1) for a given valley index and spin projection. The effect of the Zeeman interaction between the electron spin and the magnetic field can be taken into account by including the term $-g\tau_z\mu_B B/2$ where τ_z is the Pauli matrix of the real spin, μ_B is the Bohr magneton, and g denotes the g-factor. For the sake of brevity, we will omit the Zeeman term in most of the formulas following and restore it when it is necessary.

B. Longitudinal conductivity

At zero temperature, the longitudinal part of the conductivity tensor for an electron gas in the presence of static disorder can be calculated using the Kubo-Bastin-Středa formula[36,37]

$$\sigma_{ii}(0,\mu) = \frac{e^2\hbar}{\pi}\left\langle \mathrm{Tr}\left[v_i \,\mathrm{Im}\, G(\mu) v_i \,\mathrm{Im}\, G(\mu)\right]\right\rangle, \tag{6}$$

where μ is a chemical potential, the velocity operator is defined as $v_i = (i/\hbar)\,[H, r_i]$, $\mathrm{Im}\, G \equiv (i/2)\left[G^{(+)} - G^{(-)}\right]$, and $G^{(\pm)}(\epsilon)$ denotes $(\epsilon - \mathcal{H} \pm i\delta)^{-1}$. Here, $\mathcal{H} = H + V_{\mathrm{imp}}$ is a total Hamiltonian which includes an impurity potential V_{imp} (specified later). The angle brackets stand for the average over the impurity positions. As was shown previously, in the case of short-ranged scatterers the current vertex corrections in Eq. (6) vanish,[25,36] and hereafter we imply that the effect of the impurities is included into the Green function self-energy. The conductivity at the finite temperature can be restored from the expression

$$\sigma_{ii}(T,\mu) = -\int_{-\infty}^{\infty} d\epsilon \frac{\partial f(\epsilon)}{\partial \epsilon}\sigma(0,\epsilon) \tag{7}$$

where $f(\epsilon) = \{1 + \exp[(\epsilon-\mu)/k_BT]\}^{-1}$ is the Fermi–Dirac distribution function with the temperature T.

Calculating the trace in Eq. (6) with respect to the Landau level eigenfunctions we obtain

$$\sigma_{ii}(0,\mu) = \frac{e^2\hbar v_F^2}{2\pi^2\ell^2}\sum_{m,n=-\infty}^{\infty} \left|\langle n|\bar{v}_i|m\rangle\right|^2 \mathcal{A}_n(\mu)\mathcal{A}_m(\mu), \tag{8}$$

where $i = x, y$,

$$\bar{v}_x = \sigma_x \quad \text{and} \quad \bar{v}_y = \sigma_y + \eta, \tag{9}$$

and

$$\mathcal{A}_n(\mu) = \frac{\Gamma(\mu)}{\left(\mu - E_n - R(\mu)\right)^2 + \Gamma^2(\mu)}. \tag{10}$$

We imply that the electron self-energy $\Sigma(\mu) \equiv R(\mu) + i\Gamma(\mu)$ is free of the Landau level index dependence. Here, σ_{ii} denotes the conductivity per valley and per one spin projection. The Zeeman interaction in Eq. (8) can be easily restored by the substitution $\sigma_{ii}(0,\mu) \to \sigma_{ii}(0,\mu + \frac{g}{2}\mu_B B) + \sigma_{ii}(0,\mu - \frac{g}{2}\mu_B B)$.

The matrix elements of the velocity operators can be calculated explicitly

$$\langle m|\bar{v}_x|n\rangle = -i\lambda\Delta_{n,-m}P_m^n(\eta\Delta_{n,m}), \tag{11}$$

$$\langle m|\bar{v}_y|n\rangle = \lambda^2\Delta_{n,m}P_m^{-n}(\eta\Delta_{n,m}), \tag{12}$$

where $n \neq m$, $\Delta_{n,m} = \mathrm{sgn}(n)\sqrt{|n|} - \mathrm{sgn}(m)\sqrt{|m|}$,

$$P_m^n(\eta\Delta_{n,m}) = \frac{1}{\sqrt{(2-\delta_{n0})(2-\delta_{m0})}}\sqrt{\frac{|m|!}{|n|!}}\exp\left(-\frac{1}{2}\eta^2\Delta_{n,m}^2\right)(\eta\Delta_{n,m})^{|n|-|m|-1} \times\left(L_{|m|}^{|n|-|m|}(\eta^2\Delta_{n,m}^2) - \mathrm{sgn}(n)\,\mathrm{sgn}(m)\sqrt{\frac{|n|}{|m|}}L_{|m|-1}^{|n|-|m|}(\eta^2\Delta_{n,m}^2)\right), \tag{13}$$

and $L_m^\alpha(x)$ denotes the generalized Laguerre polynomial. The matrix elements of velocity operators with $n = m$ equal to zero. The details of the derivation are given in Appendix A.

For simplicity of the subsequent analysis, we introduce dimensionless conductivities in the direction perpendicular $\sigma_\perp = \sigma_{xx}/\left(\frac{e^2}{\pi\hbar}\right)$ and parallel $\sigma_\parallel = \sigma_{yy}/\left(\frac{e^2}{\pi\hbar}\right)$ to the tilting where $h = 2\pi\hbar$. The dimensionless conductivities can be written as functions of dimensionless parameters

$$\sigma_\perp(x) = \frac{1}{2\lambda}\sum_{n,m}\Delta_{n,-m}^2\left[P_m^n(\eta\Delta_{n,m})\right]^2 g_m(x)g_n(x), \tag{14}$$

$$\sigma_\parallel(x) = \frac{\lambda}{2}\sum_{n,m}\Delta_{n,m}^2\left[P_m^{-n}(\eta\Delta_{n,m})\right]^2 g_m(x)g_n(x), \tag{15}$$

where

$$g_n(x) = \frac{\gamma}{(x - \mathrm{sgn}(n)\sqrt{|n|})^2 + \gamma^2}, \tag{16}$$

$x = (\mu - R(\mu))/(\hbar\omega_c^*)$, $\gamma = \Gamma(\mu)/(\hbar\omega_c^*)$, and $\hbar\omega_c^* \equiv \lambda^{3/2}\hbar\omega_c$ is a cyclotron energy $\hbar\omega_c = \sqrt{2e\hbar v_F^2 B}$ renormalized by the tilting.

In the $\eta = 0$ limit the velocity operators in Eqs. (11) and (12) have matrix elements only for Landau levels with $|n| = |m| \pm 1$, and the expressions for the conductivities in Eqs. (14) and (15) are considerably simplified. The conductivity becomes isotropic $\sigma_\parallel = \sigma_\perp = \sigma_0$ where

$$\sigma_0(x) = \frac{\hbar\omega_c}{4} \sum_{\alpha\alpha'=\pm1} \sum_{n=0}^{\infty} \frac{\gamma}{(x - \alpha\sqrt{n+1})^2 + \gamma^2} \times \frac{\gamma}{(x - \alpha'\sqrt{n})^2 + \gamma^2}. \tag{17}$$

The summation over the Landau levels in this case can be done analytically,[27] which gives

$$\sigma_0(x) = 1 - \frac{x^2+\gamma^2}{1+16x^2\gamma^2}\left[\frac{x^2 + 4x^2\gamma^2 + 8x^2\gamma^2(x^2+\gamma^2)}{(x^2+\gamma^2)^2} - 4x\gamma\,\mathrm{Im}\,\psi\left((\gamma + ix)^2\right)\right]. \tag{18}$$

The details are given in Appendix B. In the case when $R(\mu) = 0$ and $\Gamma(\mu)$ is a constant (constant damping approximation), the conductivity at low magnetic field can be approximated using the expansion $\psi(z) = \log z - 1/(2z) - 1/(12z^2) + \ldots$ which yields

$$\sigma_{xx}(0,\mu) \approx \frac{e^2}{\pi h}\left[\Phi_0\left(\frac{\mu}{\Gamma}\right) - \frac{(\hbar\omega_c)^4}{32\Gamma^4}\Phi_2\left(\frac{\mu}{\Gamma}\right)\right], \tag{19}$$

where $\Phi_0(x)$ and $\Phi_2(x)$ are defined by

$$\Phi_0(x) = \frac{1}{2}\left[1 + \left(x + \frac{1}{x}\right)\tan^{-1} x\right], \tag{20}$$

and

$$\Phi_2(x) = -\frac{1}{x^2}\left[\frac{1-x^2}{1+x^2} - \frac{1+x^2}{x}\tan^{-1} x + \frac{8x^2(1-x^2)}{3(1+x^2)^3}\right]. \tag{21}$$

The expression for Φ_0 is well known.[25,27] In the $|x| \gg 1$ limit, we obtain $\Phi_0 \approx \pi|x|/2$, $\Phi_2 \approx \pi/(2|x|)$, while $\Phi_0 = 1 + x^2/3$, $\Phi_2 = 128x^2/15$ for $x \ll 1$.

C. Self-consistent Born approximation

In order to take into account the effect of scattering on the impurities in a self-consistent manner, we consider the total Hamiltonian in the form of $\mathcal{H} = H + V_{\mathrm{imp}}$ where

$$V_{\mathrm{imp}} = u\sum_j \delta\left(\boldsymbol{r} - \boldsymbol{R}_j\right) \tag{22}$$

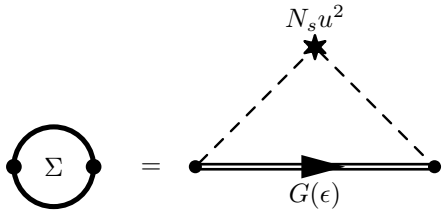

Figure 1. Diagrammatic representation of Eq. (23). Each dashed line on the right-hand side stands for $u\delta(\boldsymbol{r} - \boldsymbol{R}_j)$ and the star means the average over $\boldsymbol{R}_j$ and summation over j.

describes the interaction between the conduction electrons and randomly distributed point-like impurities at the positions $\boldsymbol{R}_j$ with the scattering potential u. Here, we imply that the impurity potential does not mix the valleys, which corresponds to the case of short-ranged scatterers in Ref. 25. The self-energy $\Sigma(\epsilon)$ in SCBA can be calculated using the method developed by Bastin *et al.*[36] and Shon and Ando[25] which leads to the self-consistent equation $\Sigma(\epsilon) = N_s u^2 V^{-1}\,\mathrm{Tr}\,G(\epsilon)$ illustrated in Fig. 1. The explicit form for this equation reads

$$\Sigma(\epsilon) = \frac{N_s u^2}{2\pi\ell^2}\sum_{n=-\infty}^{\infty}\frac{1}{\epsilon - E_n - \Sigma(\epsilon)}. \tag{23}$$

where N_s is the impurity concentration. Here, we ignore the effect of the Zeeman interaction for simplicity which is discussed below.

In zero magnetic field, we can replace the summation over the Landau levels in Eq. (23) by integration. In the Boltzmann limit, where we neglect the real part of $\Sigma(\epsilon)$ and suppose that $\Gamma(\epsilon) = \mathrm{Im}\,\Sigma(\epsilon)$ is negligible, we obtain[25]

$$\Gamma(\epsilon) = \frac{\pi\varkappa}{\lambda^3}|\epsilon|, \tag{24}$$

where $\varkappa = N_s u^2/(2\pi v_F^2\hbar^2)$ is a dimensionless parameter. The only difference of Eq. (24) from the case of $\eta = 0$ is the appearance of the factor λ^{-3} which comes from the angular dependence of the density of states at the Fermi level[19,30]

$$\int_0^{2\pi}\frac{d\phi}{2\pi}\frac{1}{(1-\eta\sin\phi)^2} = \frac{1}{(1-\eta^2)^{3/2}} = \frac{1}{\lambda^3}. \tag{25}$$

In the opposite limit, when $\epsilon \to 0$ first, we obtain $\Gamma(0) = E_c\exp\left[-\lambda^3/(2\varkappa)\right]$ where we introduced the cutoff energy E_c to regularize the logarithmic divergence. The only difference of this result from $\eta = 0$ case studied in Ref. 25 is the factor λ^3.

In the quantizing magnetic field, when $\epsilon \approx E_N$, we can keep in Eq. (23) only the contribution with $n = N$. In this case, $\Gamma(\epsilon)$ is approximated as[25]

$$\Gamma(\epsilon) = \frac{\hbar\omega_c\sqrt{\varkappa}}{\sqrt{2}}\sqrt{1 - \frac{2}{\varkappa}\frac{(\epsilon - E_N)^2}{(\hbar\omega_c)^2}}. \tag{26}$$

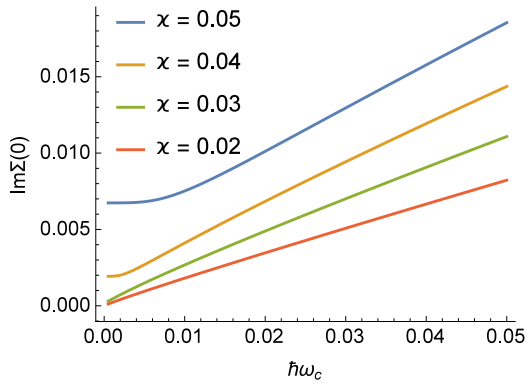

Figure 2. (Color online) $\mathrm{Im}\,\Sigma(\epsilon)$ at $\epsilon = 0$ as a function of $\hbar\omega_c$ for several $\varkappa$ with $E_c = 1$ and $\eta = 0$.

In finite magnetic fields, in order to have a convenient analytic expression for Eq. (23), we rewrite it in the following form:

$$\Sigma(\epsilon) = N_s u^2 \int_{-\infty}^{\infty} d\omega \frac{D_0(\omega)}{\epsilon - \omega - \Sigma(\epsilon)} \tag{27}$$

where

$$D_0(\omega) = \frac{1}{4\pi\ell_B^2} \sum_{n=-\infty}^{\infty} \delta\left(\omega - E_n\right) \tag{28}$$

is the density of states in the absence of the impurities. Equation (27) contains a divergence which can be treated analytically using the convenient representation for $D_0(\omega)$ obtained in Ref. 38:

$$D_0(\omega) = \frac{1}{4\pi\ell_B^2} \mathrm{sgn}\,\omega \frac{d}{d\omega} \left\{ \theta(\omega^2) \left[\frac{\omega^2}{(\hbar\omega_c^*)^2} + \frac{1}{\pi} \tan^{-1} \cot \frac{\pi\omega^2}{(\hbar\omega_c^*)^2} \right] \right\}. \tag{29}$$

Now the integration in Eq. (27) can be performed explicitly which finally gives the self-consistent equation

$$\frac{\Sigma}{\hbar\omega_c^*} = -\frac{\varkappa}{\lambda^3} \Phi\left(\frac{\mu - \Sigma}{\hbar\omega_c^*}; \frac{E_c}{\hbar\omega_c^*} \right) \tag{30}$$

where

$$\Phi(x;\epsilon_c) = x \left[\log\left(\epsilon_c^2 - x^2\right) - \psi(x^2) - \frac{1}{2x^2} - \pi \cot(\pi x^2) \right]. \tag{31}$$

The effect of the Zeeman splitting can be introduced in Eq. (30) by changing the right-hand side to

$$\sum_{\sigma=\pm 1} \Phi\left(\frac{\mu - \Sigma - \frac{g}{2}\sigma\mu_B B}{\hbar\omega_c^*}; \frac{E_c}{\hbar\omega_c^*} \right). \tag{32}$$

The ϵ dependence of $\mathrm{Im}\,\Sigma(\epsilon)$ was studied in Ref. 25. In Fig. 2, we show how $\mathrm{Im}\,\Sigma(\epsilon)$ depends on the cyclotron energy at $\epsilon = 0$. In order to obtain Fig. 2, we solved Eq. (30) numerically with fixed $E_c = 1$. At $\hbar\omega_c = 0$ the value of $\mathrm{Im}\,\Sigma(0)$ for small $\varkappa$ becomes exponentially small in agreement with the expression $E_c \exp\left[-\lambda^3/(2\varkappa)\right]$. For large enough cyclotron energy, the dependence becomes linear which corresponds to $\Gamma(0) \sim B^{1/2}$. In the following, we will denote

$$\Gamma(B) = \mathrm{Im}\,\Sigma(0) \sim \sqrt{B} \tag{33}$$

obtained in SCBA in order to distinguish it from the constant Γ.

III. CONDUCTIVITY AT ZERO TEMPERATURE

In this section, we analyze the effect of the tilting on the zero temperature conductivity in high magnetic fields where the Landau quantization of the energy spectrum plays the principal role. At fist, we analyze the chemical potential dependence of the conductivity using Eqs. (14) and (15). After that, we give a clear physical explanation of the conductivity at the Nth Landau level and discuss its relation for the quasi-classical picture. Second, we numerically study how the conductivity at the Dirac point depends on magnetic field and impurity concentration. The results are given for two models of the impurity scattering: constant broadening approximation and SCBA.

A. High magnetic fields

We start with analyzing the conductivity at $T = 0$ in the high magnetic field when Landau levels are well separated ($\hbar\omega_c \gg \Gamma(\mu)$). In this case, when the chemical potential is close to E_N we can keep only the terms with $n = N$ in the summation in Eqs. (14) and (15) which gives

$$\sigma_l(\mu) = \sigma_N^{(l)} \frac{\Gamma_N^2(\mu)}{\left(\mu - E_N\right)^2 + \Gamma_N^2(\mu)}, \tag{34}$$

where $l = (\perp, \parallel)$. The coefficients $\sigma_N^{(l)}$, which are $\sigma_l(\mu)$ at $\mu = E_N$, are defined by

$$\sigma_N^{(\perp)} = \frac{e^2}{\pi h\lambda} \sum_{m\neq N} \frac{\Delta_{N,-m}^2}{\Delta_{N,m}^2} \left[P_N^m(\eta\Delta_{N,m})\right]^2, \tag{35}$$

$$\sigma_N^{(\parallel)} = \frac{e^2\lambda}{\pi h} \sum_{m\neq N} \left[P_N^{-m}(\eta\Delta_{N,m})\right]^2. \tag{36}$$

For the constant broadening approximation the conductivity in the vicinity of the Nth Landau level is given by

$$\sigma_l(\mu) = \sigma_N^{(l)} \frac{\Gamma^2}{\left(\mu - E_N\right)^2 + \Gamma^2}, \tag{37}$$

while if we use Eq. (26) for Γ_N in SCBA, the expression for the conductivity becomes

$$\sigma_l(\mu) = \sigma_N^{(l)} \left[1 - \frac{2}{\varkappa} \frac{(\mu - E_N)^2}{(\hbar\omega_c)^2} \right]. \tag{38}$$

Note that $\sigma_N^{(l)}$ does not depend on $\Gamma(\mu)$, and the difference between constant Γ and SCBA appears only in the μ-dependence of $\sigma_l(\mu)$.

The $\eta = 0$ case was studied by Shon and Ando[25] who showed that $\sigma_N^{(l)} = \frac{e^2}{\pi\hbar}(\delta_{N0} + 2|N|)$. For finite η, using the numerical summation over Landau levels in Eqs. (35) and (36), we have found similar results

$$\sigma_N^{(\perp)} = \frac{e^2}{\pi h\lambda} \left(\delta_{N0} + 2|N| - N\eta^2 \right), \tag{39}$$

$$\sigma_N^{(\parallel)} = \frac{e^2\lambda}{\pi h} \left(\delta_{N0} + 2|N| \right). \tag{40}$$

Note that for $N = 0$, these equations can be verified explicitly using Eq. (13),

$$\lambda\sigma_{N=0}^{(\perp)} = \lambda^{-1}\sigma_{N=0}^{(\parallel)} \sim \sum_{n=1}^{\infty} \frac{\left(\eta^2 n\right)^{n-1}}{n!} e^{-\eta^2 n} = 1. \tag{41}$$

while for $|N| > 1$ the expansions (B7) and (B11) allow to confirm these equations up the order of η^2.

From Eqs. (39) and (40) we find out that both $\sigma_\perp$ and $\sigma_\parallel$ are modified by the tilting through the factors λ^{-1} and λ, respectively, which can be accounted for the geometrical modification of the quasi-classical electron orbit (discussed below). However, $\sigma_\perp$ has an additional modification by the tilting for $N \neq 0$ as demonstrated in Fig. 3, where the normalized conductivities $\tilde{\sigma}_\parallel = \lambda^{-1}\sigma_\parallel$ and $\tilde{\sigma}_\perp = \lambda\sigma_\perp$ are shown as functions of μ calculated numerically in SCBA using the summation over 50 Landau levels in Eqs. (14) and (15).

The reason why $\tilde{\sigma}_\parallel$ at $\mu = E_N$ remains the same as in the $\eta = 0$ case, while $\tilde{\sigma}_\perp$ is reduced by $N\eta^2/\lambda$ can be understood as follows. From the Eq. (8), the conductivity at $\mu = E_N$ can be expressed as

$$\sigma_N^{(l)} = \frac{e^2\hbar}{\pi^2\ell^2} \sum_m{}' \frac{\langle N|v_l|m\rangle \langle m|v_l|N\rangle}{(E_N - E_m)^2} \tag{42}$$

where the prime indicates that the $m = N$ term is omitted. Using the relation $v_l = (i/\hbar)[H, r_l]$, we can write the off-diagonal matrix elements of the velocity operator as

$$\langle N|v_l|m\rangle = \frac{i}{\hbar} (E_N - E_m) \langle N|r_l|m\rangle \tag{43}$$

which gives

$$\sigma_N^{(l)} = \frac{e^2}{\pi^2\hbar} \frac{\langle (\Delta r_l)^2 \rangle_N}{\ell^2} \tag{44}$$

where $\langle (\Delta r_l)^2 \rangle_N \equiv \langle N|r_l^2|N\rangle - \langle N|r_l|N\rangle^2$. Even in the presence of the tilting, the zero-temperature conductivity

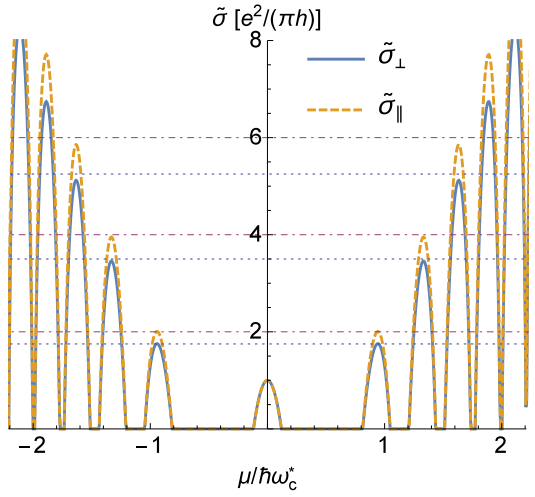

Figure 3. (Color online) Chemical potential dependence of the normalized conductivities $\tilde{\sigma}_\parallel = \lambda^{-1}\sigma_\parallel$ and $\tilde{\sigma}_\perp = \lambda\sigma_\perp$ in SCBA with $\eta = 0.5$, $\varkappa = 0.005$, and $E_c/\hbar\omega_c^* = 100$. The dotted-dashed (dotted) horizontal line is a guide for eyes at the value $2N$ ($2N - N\eta^2$).

at $\mu = E_N$ in the quantum limit is determined only by the Nth Landau level wave function and proportional to the quantum-mechanical average of $(\Delta r_l)^2$ in the Ψ_{kN}-state.

From the semiclassical point of view, the trajectories of a Dirac electron in the momentum space with the tiling $0 < \eta < 1$ are displaced ellipses which can be parametrized as

$$k_x = b_N \sin\phi, \tag{45}$$

$$k_y = x_N\ell^{-2} + a_N \cos\phi, \tag{46}$$

with the semimajor (semiminor) axis equal to $a_N = \ell^{-1}\sqrt{2|N|/\lambda}$ ($b_N = \ell^{-1}\sqrt{2|N|\lambda}$) and $0 \leq \phi < 2\pi$. The area of each ellipse is independent of η and given by $S_N = 2\pi|N|\ell^{-2}$. Note that the Berry phase contribution to the semiclassical quantization rule $\varphi_B = \pi$, as in the case without tilting.[19] Each ellipse has its focus at the axes origin and its center displaced by $x_N\ell^{-2}$ in the k_y-direction, as shown in Fig. 4. The eccentricity of each ellipse is η. The trajectory in the real space can be obtained by rotation of the orbit in the momentum space by $\pi/2$ and rescaling it with the factor ℓ^2. If we make a semiclassical calculation of $\langle (\Delta r_l)^2 \rangle_N$, we obtain

$$\langle (\Delta x)^2 \rangle_N = \int_0^{2\pi} \frac{d\phi}{2\pi} (x - x_N)^2 = \frac{|N|}{\lambda}, \tag{47}$$

and $\langle (\Delta y)^2 \rangle_N = \lambda|N|$. The appearance of the factor λ^{-1} (λ) in the $\sigma_\perp$ ($\sigma_\parallel$) is therefore accounted for the ellipticity of the electron orbit. However, in the semiclassical picture the displacement of the orbit has no effect on the conductivity and behavior of $\sigma_\perp$ and $\sigma_\parallel$ at $\mu = E_N$ is the same as in the case of $\eta = 0$.

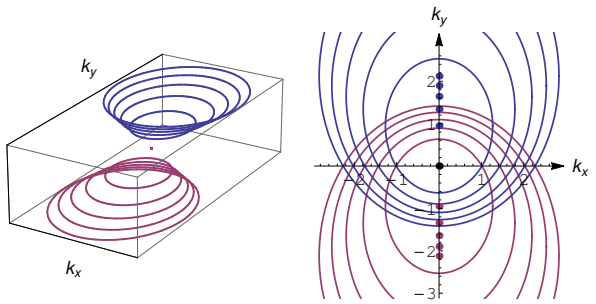

Figure 4. (Color online) Semiclassical trajectories of a massless Dirac electron with the tilted cone in the k space with $\eta = 0.6$ for $n = -5, \ldots, 5$. The units of k_x and k_y are ℓ^{-1}. The blue (purple) ellipses correspond to the upper (lower) band. The dots show centers of the ellipses. Each ellipse has its focus at the origin and its center displaced by $x_n\ell^{-2}$ in the y-direction. The eccentricity of each ellipse is η.

The quantum-mechanical average of the r_l^2 and r_l ($l = x, y$) operators calculated with respect to the eigenfunctions in Eq. (3) gives the following results:

$$\langle N|x|N\rangle = \frac{3}{2}x_N, \tag{48}$$

$$\langle N|x^2|N\rangle = 2x_N^2 + \frac{\ell^2}{2\lambda}\left(\delta_{N0} + 2|N|\right), \tag{49}$$

$$\langle N|y^2|N\rangle = \frac{\lambda\ell^2}{2}\left(\delta_{N0} + 2|N|\right), \tag{50}$$

and $\langle N|y|N\rangle = 0$ which justifies Eqs. (39) and (40) obtained by numerical calculations. These results are different from those obtained in the semiclassical picture, because $\langle N|x|N\rangle \neq x_N$. Note that according to our gauge choice, y is an unbounded operator and a regularization procedure is required. The details are given in Appendix C.

B. Magnetic-field dependence

It is well known that in the $\eta = 0$ case, the zero-temperature conductivity at $\mu = 0$ is independent of magnetic field and impurity concentration and given by the universal value $e^2/(\pi h)$.[25] The natural question is how this behavior is modified for $\eta > 0$. At zero magnetic field, we already know the answer. In our previous work, we have found that the conductivities at $\mu = 0$ are independent of the impurity broadening and defined by the following expressions:[30]

$$\sigma_\perp = \frac{1}{\sqrt{1-\eta^2}}, \tag{51}$$

$$\sigma_\parallel = \frac{\sin^{-1}\eta}{\eta}. \tag{52}$$

If we compare these results with the case of strong magnetic field given by Eqs. (37) and (38) with $N = 0$, we would find that $\sigma_\perp$ remains the same in both limiting cases $\hbar\omega_c^* \to \infty$ and $\hbar\omega_c^* \to 0$, while $\sigma_\parallel$ increases from $\sqrt{1-\eta^2} < 1$ to $\sin^{-1}\eta/\eta > 1$ as $\hbar\omega_c^*$ is reduced from ∞ to zero.

First, we analyze the behavior of the conductivity at low magnetic fields in the constant damping approximation. In order to study the behavior of the conductivities in the region of moderate magnetic fields, we have made a numerical summation in Eqs. (14) and (15) over $N = 150$ Landau levels. Figure 5 (a) shows normalized conductivities $\tilde\sigma_\perp = \lambda\sigma_\perp$ and $\tilde\sigma_\parallel = \lambda^{-1}\sigma_\parallel$ at $\mu = 0$ for moderate tilting $\eta = 0.4$ and 0.5. Note that at $\mu = 0$ the only parameter is $\Gamma/\hbar\omega_c^*$ which is proportional to $B^{-1/2}$. Within the numerical accuracy we found that $\tilde\sigma_\perp$ remains constant with increasing $\Gamma/\hbar\omega_c^*$ and does not depend on η, while $\tilde\sigma_\parallel$ increases with increasing Γ or η, but remains smaller than the corresponding limiting value $\sin^{-1}\eta/(\lambda\eta)$ shown by dashed lines. Note that for large values of η, numerical calculations become complicated especially due to the inter-band matrix elements of velocity operators with large $|m|$ and $|n| - |m|$ [see Eq. (13)].

Second, we show the normalized conductivities in SCBA in Fig. 5(b) where Eq. (30) has been used. For the self-consistent calculation we kept $E_c/\hbar\omega_c^*$ fixed and varied parameter $\varkappa$ which is proportional to the total number of impurities. In SCBA, the behavior of the conductivities in the crossover region remains qualitatively the same as discussed above. As $\varkappa$ increases, within the numerical accuracy $\tilde\sigma_\perp$ remains constant, while $\tilde\sigma_\parallel$ increases, but remains below the limiting value at zero field (which is the same in both constant broadening and SCBA cases).

At the end of this section, we comment about the difference between the anisotropy of the conductivity given by the tilting and the anisotropy due to the difference of Fermi velocities $v_x \neq v_y$ in the x and y-directions. In the latter case, the energy spectrum is[19] $E_n = \mathrm{sgn}(n)v_F^*\sqrt{2eB\hbar|n|}$, where $v_F^* = \sqrt{v_x v_y}$. The quasi-classical orbits are ellipses centred at the axes origin with the eccentricity defined by $\sqrt{v_x/v_y}$. Equation (44), in this case, gives the same conductivities at $\mu = E_N$ as in the isotropic case renormalized by the factor v_x/v_y (v_y/v_x) for σ_{xx} (σ_{yy}), which coincides with the conductivities obtained by the quasi-classical argument. Note that in the case of the anisotropy induced by $v_x \neq v_y$, the ratio $\sigma_{xx}/\sigma_{yy} = v_x^2/v_y^2$ is independent of the magnetic field (zero-field case was considered in Ref. 30), while if the anisotropy is produced by the tilting, σ_{xx}/σ_{yy} changes from $\sin^{-1}\eta/(\eta\lambda)$ in zero field to λ^{-2} in the high-field limit. The magnetic-field-dependent anisotropy of the in-plane conductivity which saturates in the quantum limit can be used as an evidence of the tilting in Dirac electron systems with μ close to the Dirac point.

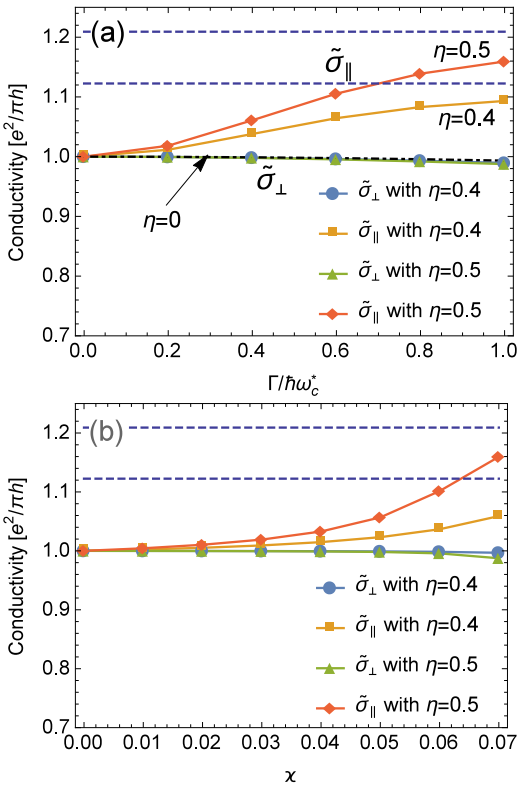

Figure 5. (Color online) Normalized conductivities $\tilde{\sigma}_\parallel = \lambda^{-1}\sigma_\parallel$ and $\tilde{\sigma}_\perp = \lambda\sigma_\perp$ at $\mu = 0$ with $\eta = 0.4$ and 0.5 calculated from Eqs. (14) and (15) numerically using $N = 150$ Landau levels. (a) The conductivities in the constant broadening approximation as functions of $\Gamma/\hbar\omega_c^*$; $\eta = 0$ case is indicated by the dotted-dashed line. (b) The conductivities in SCBA as functions of $\varkappa$ with $E_c/\hbar\omega_c^* = 100$. In each figure, the upper (lower) dashed line corresponds to the limiting value $\sin^{-1}\eta/(\lambda\eta)$ at zero field for $\eta = 0.5$ ($\eta = 0.4$).[30]

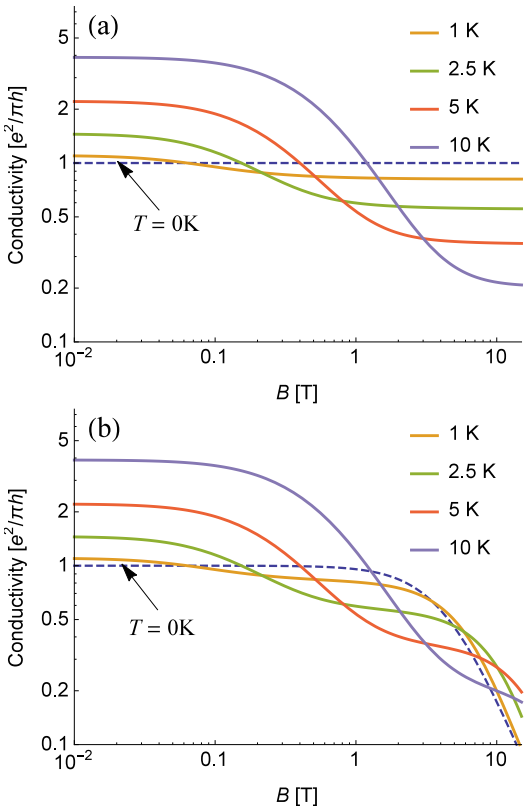

Figure 6. (Color online) Magnetic-field dependence of the conductivity at $\mu = 0$ in the constant broadening approximation for several temperatures without the Zeeman interaction (a) and with the Zeeman interaction included (b).

IV. CONDUCTIVITY AT FINITE TEMPERATURES

In the following, we discuss the magnetic-field dependence at finite temperature and the temperature dependence of the conductivity and the resistivity at $\mu = 0$ which can be directly compared with experiments.[4,33,34] The experimental measurements of the magnetic-field dependence of the in-plane conductivity in α-(BEDT-TTF)$_2$I$_3$ organic conductor demonstrated a two-step decrease of the conductivity with increasing the magnetic field.[33,34] In Ref. 33 this two-step decrease was interpreted in terms of quasi-classical two-carrier model, where Dirac carriers and massive carriers coexist. Similar two-step behavior of the conductivity was also reported in Ref. 34. However, in Ref. 34 detailed analysis of the magnetic-field dependence with fixed T revealed the existence of a novel minimum in the conductivity at a moderate magnetic field which scales as T^2 in the temperature range of 1.5 K $< T <$ 5 K. In this section, taking account of the recent experiment,[34] we show an alternative explanation for the two-step behavior in terms of one carrier scenario of Dirac electrons. Furthermore, in the present explanation, the minimum of conductivity can be understood. At first, we consider the constant damping approximation which is frequently used in the literature.[12,27,28,32,38] Secondly, we show how the results obtained in the constant damping approximation are modified if SCBA for the impurity scattering is used. We start with analyzing $\eta = 0$ case in detail, and, after that, the effect of the tilting is considered.

Hereafter, parameters are chosen with respect to the application to α-(BEDT-TTF)$_2$I$_3$:[8] $v_F = 5 \times 10^4$ m/s, $\Gamma/k_B = 3$ K, and $g = 2$, if these values are not indicated explicitly.

A. Conductivity in constant damping approximation

In this section, we consider a simple case where the self-energy has the form $\Sigma(\epsilon) = i\Gamma$, with Γ being a phenomenological parameter. Magnetic-field dependence of the conductivity calculated from Eqs. (7) and (18) for $\mu = 0$ and $\eta = 0$ is shown in Fig. 6. Figure 6(a) shows the result without the Zeeman interaction and 6(b) with

the Zeeman interaction. First, we discuss the case without the Zeeman interaction [Fig. 6(a)]. We interpret that the decrease of σ is associated with the crossover from the low magnetic-field region where Landau levels overlap to the quantum region where Landau levels are well separated. Actually, this crossover occurs when $\hbar\omega_c \sim k_B T$. In the limit of $B \to \infty$, the conductivity saturates at the value determined by the $n = 0$ Landau level.

Next, we discuss the temperature dependence. The effect of the temperature on the conductivity is the opposite in low and high magnetic fields. In the low-field region, increasing of the temperature enhances the conductivity. This will be due to the thermal activation of the carriers. In contrast, in the quantum region, increasing the temperature reduces the conductivity. This is because the $n = 0$ Landau level has a temperature smearing and, as a result, reduces the conductivity.

At low temperatures, the crossover in Fig. 6 (a) between the low magnetic-field region and high magnetic-field region can be discussed analytically from Eqs. (7) and (18). We can use the Sommerfeld expansion for the Fermi–Dirac distribution $-\partial f/\partial\epsilon = \delta(\epsilon-\mu) + (\pi^2 k_B^2 T^2/6)\delta''(\epsilon-\mu)$ which gives

$$\sigma(T) = \frac{e^2}{\pi h}\left(1 + \frac{\pi^2 k_B^2 T^2}{6\Gamma^2}\sigma''(0)\right), \tag{53}$$

where $\sigma''(0) = d^2\sigma(0)/d(\mu/\Gamma)^2$ defined at $\mu = 0$. $\sigma''(0)$ can be found analytically from Eq. (18)

$$\sigma''(0) = -2\left[1 + 4\gamma^2 + 8\gamma^4 - 8\gamma^6\psi'(\gamma^2)\right]. \tag{54}$$

In large magnetic field ($\gamma \ll 1$), $\sigma''(0) \to -2$, and the conductivity in Eq. (53) approaches $\frac{e^2}{\pi h}(1-\pi^2 k_B^2 T^2/3\Gamma^2)$. This explains the increase of $\sigma(T)$ as a function of T in high magnetic fields. When the magnetic field decreases, $\sigma(T)$ reaches the universal value $e^2/(\pi h)$ at $\hbar\omega_c/\Gamma \approx 1.30$ which gives zero for the right-hand side in Eq. (54), and roughly represents the crossover between low-field and high-field regions. At low magnetic fields ($\gamma \gg 1$), $\sigma''(0) \approx \frac{2}{3} - \frac{8}{15}\gamma^{-4}$, and the behavior of the conductivity is given by

$$\sigma(T) \approx \frac{e^2}{\pi h}\left[1 + \frac{\pi^2 k_B^2 T^2}{9\Gamma^2}\left(1 - \frac{4}{5}\frac{(\hbar\omega_c)^4}{\Gamma^4}\right)\right]. \tag{55}$$

This explains the increase of $\sigma(T)$ as a function of T in low magnetic field.

Next, we discuss the effect of the Zeeman interaction in Fig. 6 (b). When we include the Zeeman term there appears the second step decrease in the high magnetic field due to the opening of the gap at $\mu = 0$. The magnetic-field dependence of the conductivity in this region can be understood as follows. At zero temperature, the conductivity per spin near $\mu = 0$ in the spin-splitting region can be approximated as

$$\sigma(0,\mu) = \frac{e^2}{2\pi h}\sum_{s=\pm 1}\frac{\Gamma^2}{(\mu + gs\mu_B B/2)^2 + \Gamma^2}. \tag{56}$$

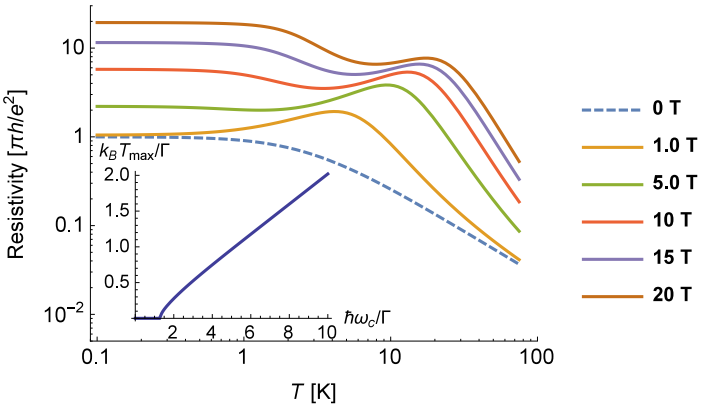

Figure 7. (Color online) Temperature dependence of the resistivity at $\mu = 0$ for several magnetic fields. The dashed line shows the resistivity at zero magnetic field. The inset shows the position of the maximum $k_B T_{\max}$ as a function of $\hbar\omega_c$ with $g = 0$.

At $\mu = 0$

$$\sigma(0,0) = \frac{e^2}{\pi h}\frac{1}{1 + (g\mu_B B/2\Gamma)^2}. \tag{57}$$

This expression indicates that $\sigma(0,0)$ decreases when $g\mu_B B > 2\Gamma$. At finite temperatures, $\sigma(T)$ is obtained by Eq. (7). In this case, $\sigma(T)$ starts to decrease for sufficiently large magnetic field $2\mu_B B > k_B T$.

Finally, we discuss the temperature dependence of the resistivity. Figure 7 shows $\rho(T,0)$ for several magnetic fields. The characteristic feature of resistivity in Fig. 7 is the maximum in the temperature dependence which separates the high-temperature region ($k_B T \gg \hbar\omega_c$) from the low-temperature region ($k_B T \ll \hbar\omega_c$). In the high-temperature region, the resistivity is determined by the thermal activation of the carriers, which leads to the increase of the resistivity with lowering the temperature. In the low-temperature region, where the $n = 0$ level becomes isolated, the behavior of the resistivity is the opposite, since increasing the temperature reduces the density of states at $\mu = 0$ due to the temperature broadening. Therefore, resistivity takes the maximum at $k_B T_{\max} \sim \hbar\omega_c$. The result of the numerical calculation of $T_{\max}$ on the $(\hbar\omega_c, k_B T)$-plane is presented in the inset in Fig. 7, which shows that at high $\hbar\omega_c$, $k_B T_{\max} \approx 0.21(\hbar\omega_c - 0.5\Gamma)$. In low magnetic fields, the maximum disappears when $\hbar\omega_c \approx 1.30\,\Gamma$, which also gives zero for the right-hand side in Eq. (54).

B. Conductivity in SCBA

In this section, we discuss how SCBA modifies the results obtained in the previous section. The main feature in SCBA is that the level broadening $\Gamma(B)$ increases as $\sqrt{B}$.[25] As a result, the behavior of σ changes when

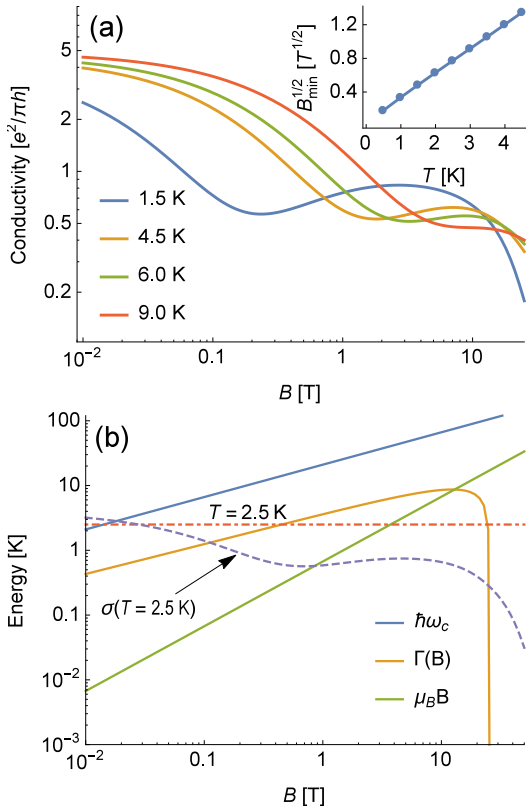

Figure 8. (Color online) (a) Magnetic-field dependence of the conductivity at $\mu = 0$ in SCBA for several temperatures with $\varkappa = 0.02$ and $E_c = 0.05$ eV. The inset shows $B_{\rm min}^{1/2}$ vs temperature. (b) Magnetic-field dependence of $\hbar\omega_c$, $\Gamma(B)$, $\mu_B B$, and the conductivity in the unit of $e^2/\pi h$ at $T = 2.5$ K (dashed line) in the same plot. The horizontal dotted-dashed line corresponds to $T = 2.5$ K.

$\Gamma(B) \sim k_B T$. This leads to a minimum of the conductivity which is the central result in this section.

Figure 8(a) shows the conductivity for $\mu = 0$ and $\eta = 0$ with the Zeeman interaction as a function of the magnetic field in SCBA for several temperatures, where the self-energy was calculated numerically from Eq. (30). In contrast to the simple two-step decrease in Fig. 6(b), the conductivity in SCBA takes a minimum in the moderate magnetic field region. We find that this minimum is due to the crossover between the "temperature-dominating" [$\Gamma(B) \lesssim k_B T$] and "impurity-dominating" [$k_B T \lesssim \Gamma(B)$] regimes. In order to explain this, we show the energy scales of our problem, i. e., $\hbar\omega_c$, $\Gamma(B)$ [Eq. (33)], $\mu_B B$, and $k_B T$ (dotted-dashed line) in Fig. 8(b). The dashed line is the conductivity for $T = 2.5$ K as a function of B. We can see that the minimum of σ occurs at $\Gamma(B) \sim k_B T$. In the low-magnetic field region, $\Gamma(B)$ is smaller than $k_B T$, which corresponds to the temperature dominating region. In this case, σ decreases according to Eq. (55). On the other hand, when $\Gamma(B) > k_B T$, the conductivity slightly increases. This is because σ can be approximated from Eqs. (53) and (54) as $\sigma = 1 - \pi^2 k_B^2 T^2 / 3\Gamma^2(B)$ which approaches 1 with increasing $\Gamma(B)$. Then, in the high-magnetic field region, $\Gamma(B)$ starts to decrease, and, as a result, σ decreases due to the Zeeman interaction.

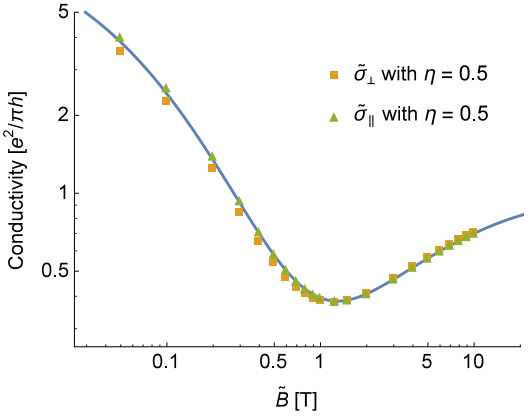

Figure 9. (Color online) Magnetic-field dependence of the conductivity at $\mu = 0$ in SCBA for $T = 4.5$ K, $\varkappa = 0.02$, and $E_c = 0.05$ eV calculated from Eqs. (18) and (30) (solid line). Closed squares (triangles) show $\tilde{\sigma}_\perp$ ($\tilde{\sigma}_\parallel$) with $\eta = 0.5$ calculated from Eqs. (7) and (14) [Eq. (15)] using summation over 30 Landau levels. The horizontal axis is renormalized as $\tilde{B} = B(1-\eta^2)^{-3/4}$.

In order to confirm this interpretation, we calculate $B_{\rm min}$ of various temperatures numerically. As shown in the inset of Fig. 8(a), $B_{\rm min}$ scales as T^2 in agreement with the relation $\Gamma(B) \sim \sqrt{B} \sim k_B T$. The minimum of σ disappears at high temperatures [e. g., "$T = 9$ K" curve in Fig. 8(a)]. This is because $k_B T > \Gamma(B)$ holds in all range of magnetic fields.

In the high-magnetic-field region where the Zeeman term reduces σ, the B dependence of σ is different from that obtained in the previous section. At $T = 0$, according to Eq. (38), we obtain

$$\sigma(0,0) = \begin{cases} \frac{e^2}{\pi h}\left(1 - \frac{B}{B_c}\right), & \text{for } B < B_c, \\ 0, & \text{otherwise,} \end{cases} \tag{58}$$

where $B_c = \varkappa e\hbar v_F^2/(g^2\mu_B^2)$. At finite temperatures, the conductivity in the region $B \gtrsim B_c$ decreases exponentially with magnetic field, $\sigma(T) \sim \exp(-\mu_B B/k_B T)$.

Next, we study how our results for the magnetic-field dependence of the conductivity are modified by the tilting of the Dirac cone. First of all, there are η-dependent prefactors of $\sigma_\perp$ and $\sigma_\parallel$ [Eqs. (39) and (40)]. We will show that the magnetic-field dependencies of $\sigma_\perp$ and $\sigma_\parallel$ are not affected so much by η except for these prefactors. Figure 9 shows the normalized conductivities $\tilde{\sigma}_\perp = \lambda\sigma_\perp$ and $\tilde{\sigma}_\parallel = \lambda^{-1}\sigma_\parallel$ as a function of B for $T = 4.5$ K and $\varkappa = 0.02$ where there is no Zeeman term. Note that the magnetic field is also renormalized by η as $\hbar\omega_c \to \lambda^{-3/2}\hbar\omega_c$. Thus, the horizontal axis in Fig. 9 is $\tilde{B} = B(1-\eta^2)^{-3/4}$. Closed squares (triangles) in Fig. 9 show $\tilde{\sigma}_\perp$ ($\tilde{\sigma}_\parallel$) calculated from Eqs. (7) and (14) [Eq. (15)] using numerical summation. The solid line is the same curve as in Fig. 8(a) for $T = 4.5$ K which is

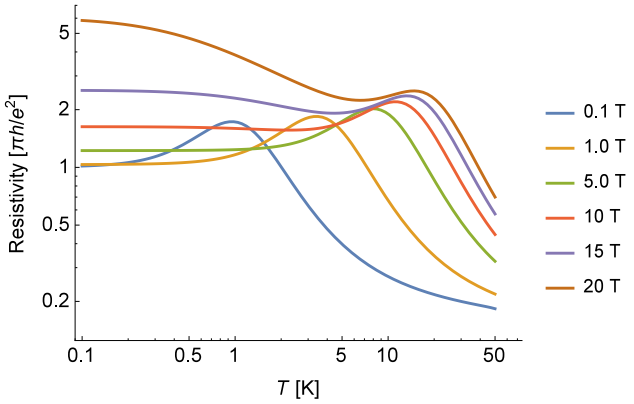

Figure 10. (Color online) Resistivity at $\mu = 0$ as a function of temperature for several magnetic fields calculated in SCBA with $\varkappa = 0.02$ and $E_c = 0.05$ eV.

shown for comparison in the case of $\eta = 0$. Figure 9 indicates that η has very small effects on the normalized conductivities. Only in the weak magnetic-field region, $\tilde{\sigma}_{\parallel}$ is slightly larger than $\tilde{\sigma}_{\perp}$. This difference can be understood in terms of Eqs. (39) and (40). In this case, there are Landau level mixings, and the contribution from higher Landau levels for $\tilde{\sigma}_{\perp}$ is smaller by the factor $N\eta^2$ than that for $\tilde{\sigma}_{\parallel}$.

The physical reason of this small η dependence will be as follows. The basic elements of our explanation for the magnetic-field dependence are the Landau level quantization and the magnetic-field dependence of the level broadening. This explanation remains qualitatively the same even if the tilting is introduced. Moreover, in the quantum limit, the conductivity is solely determined by $n = 0$ Landau level. In this case, $n = 0$ Landau level is insensitive to η except for the rescaling factors λ and λ^{-1}. This will be the reason why the tilting has very small effect on the magnetic-field dependence of the conductivity. Note that in the high-magnetic field region, where $\sigma_{\perp}$ ($\sigma_{\parallel}$) reduces due to the Zeeman splitting of $n = 0$ Landau level, the η dependence comes only through the prefactor λ^{-1} (λ).

Finally, we briefly mention the temperature dependence of the resistivity in SCBA shown in Fig. 10 for several magnetic fields. The explanation of this behavior remains qualitatively the same as in the previous section for the constant broadening approximation. The main difference of the present case from Fig. 7 is that the maximum in the temperature dependence of the resistivity survives at small magnetic fields and becomes more pronounced as magnetic field decreases. This behavior can be understood from Fig. 2 which indicates that the $n = 0$ level becomes sharper when magnetic field goes to zero, since $\Gamma(B)$ for $\varkappa = 0.02$ becomes exponentially small at $B = 0$.

V. SUMMARY

In summary, we have made an analytical calculation of the longitudinal conductivity of two-dimensional massless fermions with a tilted Dirac cone in the framework of the Kubo-Basting-Středa linear-response formula in strong magnetic field. The main difference of the present case from the case of the isotropic Dirac cone is that the tilting introduces Landau level mixing which breaks usual selection rules for the matrix elements of velocity operators which leads to the existence of matrix elements between the Landau levels with arbitrary n.

First, we have analyzed the conductivity at zero temperature in the quantized magnetic field limit. In this case, we found that the conductivities at $\mu = E_N$ are given by $\sigma_{xx} = \lambda^{-1}(\delta_{N0} + 2N - N\eta^2)$ and $\sigma_{yy} = \lambda(\delta_{N0} + 2N)$. The factors λ and λ^{-1} are purely geometrical, due to the ellipticity of the quasi-classical electron orbit. Apart from these factors, σ_{yy} remains the same as in the case without the tilting, while σ_{xx} is reduced by $N\eta^2$. We have explained this result as follows. The conductivity at $\mu = E_N$ is determined by the quantum-mechanical average of $(\Delta r_l)^2$ calculated with respect to the Nth Landau level wave function. If the tilting of the cone is in the k_y direction in the energy-momentum space, the center of the Nth eigenfunction is displaced by x_N along the x direction in the real space. We have proven that this displacement gives the reduction of $(\Delta x)^2$, while $(\Delta y)^2$ remains unchanged. We note that this fact is purely quantum effect and has no quasi-classical interpretation.

Second, we studied how the zero-temperature conductivity at $\mu = 0$ depends on magnetic field and impurity scattering. Using numerical calculations, we have demonstrated that σ_{xx} at $\mu = 0$ remains independent of magnetic field and short-ranged disorder, which is similar to the case without tilting, while σ_{yy} shows a crossover from the value $\frac{e^2}{\pi h}\frac{\sin^{-1}\eta}{\eta}$ in zero magnetic field to the value $\frac{e^2}{\pi h}\sqrt{1-\eta^2}$ in the strong-field limit. We propose that this fact can be used as an experimental evidence of the tilting of the Dirac cone. Indeed, there are two possible sources of the anisotropy of the conductivity, namely, owing to the difference in the Fermi velocities $v_x \neq v_y$, and due to the tilting. In the former case, $\sigma_{yy}/\sigma_{xx} = v_x^2/v_y^2$ does not depend on magnetic field, while in the latter case σ_{yy}/σ_{xx} changes from $\sqrt{1-\eta^2}\sin^{-1}\eta/\eta$ in zero magnetic field to $1-\eta^2$ in the high-field limit. For α-(BEDT-TTF)$_2$I$_3$ with $\eta \approx 0.8$, σ_{yy}/σ_{xx} changes, respectively, from 0.69 to 0.36 which can be detected experimentally. The magnetic-field dependent anisotropy of the in-plane conductivity can be regarded as a characteristic feature of a tilted Dirac cone.

Next, we have studied the conductivity at finite temperatures where we set $\eta = 0$ at the beginning. We have demonstrated that as a function of the magnetic field the conductivity at the Dirac point undergoes a two-step decrease where the first decrease is associated with the

crossover to the quantum limit and the second decrease is due to the spin splitting of the $n = 0$ level. For the effect of the impurities, the results are given for two models: the constant broadening approximation and SCBA. The analysis based on the SCBA shows that the broadening of the Landau levels increases with the magnetic field as $\sqrt{B}$, which leads to the minimum in the magnetoconductivity at $k_BT \sim \Gamma(B) \sim \sqrt{B_{\min}}$ which separates the temperature dominated region $k_BT \gtrsim \Gamma(B)$ from the impurity dominated region $k_BT \lesssim \Gamma(B)$. We have demonstrated that this behavior remains qualitatively the same even in the presence of the tilting of the cone.

The results of Sec IV can be directly compared with recent experiments in α-(BEDT-TTF)$_2$I$_3$ organic conductor.[33,34] We note, that in contrast with Ref. 33, our analysis is able to explain the magnetic-field dependence of the conductivity in α-(BEDT-TTF)$_2$I$_3$ using only one type of Dirac carriers. Moreover, the minimum in the magnetoconductivity, which scales with temperature as T^2, can be regarded as a strong evidence in favor of the one-carrier scenario of the magnetotransport.

In conclusion, we comment on the minor importance of the tilting of the Dirac cone for understanding the existent experiments in magnetic field in α-(BEDT-TTF)$_2$I$_3$ near $\mu = 0$. We note that the key ingredients of our explanation of the magnetic-field dependence of the conductivity, namely, the Landau quantization, the existence of the zero mode, and the magnetic-field dependence of the level broadening remain qualitatively the same even in the presence of the tilting. That is the reason why our main results in Sec. IV such as two-step behavior of the conductivity in magnetic field and the minimum in the magneto-conductivity remain valid in the presence of the finite tilting. In order to detect the effect of the tilting on the in-plane transport, the authors propose to measure the magnetic-field dependence of σ_{xx}/σ_{yy}. This effect survives at finite temperatures and can be used as a marker of a tilted cone.

ACKNOWLEDGMENTS

The authors are thankful to N. Tajima for fruitful discussions. One of the authors (Y.S.) also thanks M. Monteverde and M. O. Goerbig for useful comments. This work was supported by Grants-in-Aid for Scientific Research (A) (No. 24244053) and (C) (No. 26400355) from the Ministry of Education, Culture, Sports, Science and Technology of Japan. One of the authors (I. P.) acknowledges the Russian Foundation for Basic Research, Grant No. 14-02-92104 and the Government of the Russian Federation, Program No. 02.A03.21.0006.

Appendix A: Matrix elements of velocity operators

The matrix elements of the velocity operators in Eqs. (11) and (12) for the Landau levels in Eq. (3) can be expressed in the following form:

$$\langle m|\bar{v}_x|n\rangle = i\lambda C_{nm}\left[\mathrm{sgn}(m)F^{(01)}_{nm} - \mathrm{sgn}(n)F^{(10)}_{nm}\right], \quad \text{(A1)}$$

$$\langle m|\bar{v}_y|n\rangle = C_{nm}\left[-\eta F^{(00)}_{nm} + \mathrm{sgn}(n)F^{(10)}_{nm} + \mathrm{sgn}(m)F^{(01)}_{nm} - \eta\,\mathrm{sgn}(m)\,\mathrm{sgn}(n)F^{(11)}_{nm}\right], \quad \text{(A2)}$$

where $C_{nm} = (2-\delta_{n0})^{-1/2}(2-\delta_{m0})^{-1/2}$,

$$F^{(ij)}_{n,m} = \int_{-\infty}^{\infty} dx h_{|n|-i}(x-x_n)h_{|m|-j}(x-x_m), \quad \text{(A3)}$$

$i,j = 0,1$, and $|n| \geq i$, $|m| \geq j$. The coefficients $F^{(ij)}_{nm}$ can be calculated using the formula[39]

$$\int_{-\infty}^{\infty} e^{-x^2} H_m(x+y)H_n(x+z)dx = 2^n\pi^{1/2}m!z^{n-m}L^{n-m}_m(-2yz), \quad (m \leq n), \quad \text{(A4)}$$

which gives

$$F^{(00)}_{nm} = N^m_n L^{|n|-|m|}_{|m|}(\eta^2\Delta^2_{n,m}), \quad \text{(A5)}$$

$$F^{(10)}_{nm} = N^m_n \frac{\sqrt{|n|}}{\eta\Delta_{n,m}} L^{|n|-|m|-1}_{|m|}(\eta^2\Delta^2_{n,m}), \quad \text{(A6)}$$

$$F^{(01)}_{nm} = N^m_n \frac{\eta\Delta_{n,m}}{\sqrt{|m|}} L^{|n|-|m|+1}_{|m|-1}(\eta^2\Delta^2_{n,m}), \quad \text{(A7)}$$

$$F^{(11)}_{nm} = N^m_n \sqrt{\frac{|n|}{|m|}} L^{|n|-|m|}_{|m|-1}(\eta^2\Delta^2_{n,m}), \quad \text{(A8)}$$

where

$$N^m_n = \sqrt{\frac{|m|!}{|n|!}}\,(\eta\Delta_{n,m})^{|n|-|m|}\exp\left(-\frac{\eta^2}{2}\Delta^2_{n,m}\right), \quad \text{(A9)}$$

and we used the property of Laguerre polynomials with integer n and m:

$$\frac{(-x)^m}{m!}L^{m-n}_n(x) = \frac{(-x)^n}{n!}L^{n-m}_m(x). \quad \text{(A10)}$$

Substituting Eqs. (A5)–(A8) in the matrix elements (A1) and (A2) and using the recurrence relations for Laguerre polynomials

$$L^{|n|-|m|-1}_{|m|}(x) = L^{|n|-|m|}_{|m|}(x) - L^{|n|-|m|}_{|m|-1}(x), \quad \text{(A11)}$$

$$xL^{|n|-|m|+1}_{|m|-1}(x) = |n|L^{|n|-|m|}_{|m|-1}(x) - |m|L^{|n|-|m|}_{|m|}(x), \quad \text{(A12)}$$

we obtain the expressions (11) and (12).

Appendix B: Conductivity in the $\eta \to 0$ limit

If $\eta = 0$, the matrix elements in Eqs. (11) and (12) become

$$\langle m|\bar{v}_x|n\rangle = -iC_{nm}\left[\mathrm{sgn}(n)\delta_{|n||m|+1} - \mathrm{sgn}(m)\delta_{|m||n|+1}\right], \tag{B1}$$

$$\langle m|\bar{v}_y|n\rangle = \quad C_{nm}\left[\mathrm{sgn}(n)\delta_{|n||m|+1} + \mathrm{sgn}(m)\delta_{|m||n|+1}\right], \tag{B2}$$

where $C_{nm} = (2-\delta_{n0})^{-1/2}(2-\delta_{m0})^{-1/2}$. In this case, Eqs. (14) and (15) for the conductivities reduce to Eq. (17). In order to make a summation over n in Eq. (17), we make a summation over α and α' with the help of the identity

$$\frac{\gamma}{(x-\alpha\sqrt{n})^2+\gamma^2} = \frac{1}{2i}\left(\frac{1}{x-\alpha\sqrt{n}-i\gamma} - \frac{1}{x-\alpha\sqrt{n}+i\gamma}\right), \tag{B3}$$

which yields

$$\sigma_0(x) = \frac{1}{4}\sum_{n=0}^{\infty}\left(\frac{\gamma_+}{n+1+\gamma_+^2} + \frac{\gamma_-}{n+1+\gamma_-^2}\right)\left(\frac{\gamma_+}{n+\gamma_+^2} + \frac{\gamma_-}{n+\gamma_-^2}\right) \tag{B4}$$

where we introduced a shorthand notation $\gamma_\pm = (\gamma \pm ix)/\hbar\omega_c$. Now the summation over n can be easily done with the help of the formula

$$\sum_{n=0}^{\infty}\frac{1}{(n+a)(n+b)} = \frac{1}{b-a}\left[\psi(b)-\psi(a)\right], \tag{B5}$$

where ψ denotes digamma function. The final result is

$$\sigma_0(x) = \frac{1}{2}\left[1 + \frac{\gamma_+^2+\gamma_-^2+(\gamma_+^2-\gamma_-^2)^2}{2\gamma_+\gamma_-\left(1-(\gamma_+^2-\gamma_-^2)^2\right)} - \frac{\gamma_+\gamma_-\left(\gamma_+^2-\gamma_-^2\right)}{1-(\gamma_+^2-\gamma_-^2)^2}\left(\psi(\gamma_+^2)-\psi(\gamma_-^2)\right)\right] \tag{B6}$$

which gives Eq. (18).

In the limit $\eta\Delta_{n,m} \to 0$ we can expand Eqs. (11) and (12) in powers of η. Up to the order of η^2, v_x and v_y have matrix elements up to $|m| = |n| \pm 3$. The expansion has the form

$$\langle m|\bar{v}_x|n\rangle = i\lambda C_{nm}\sum_{j=1}^{3}\left[a_n^{(j)}\delta_{|m|=|n|+j} - a_m^{(j)}\delta_{|n|=|m|+j}\right] + O(\eta^3), \tag{B7}$$

where

$$a_n^{(1)} = \mathrm{sgn}(m)\left\{1 - \frac{1}{2}\left(\sqrt{|n|+1} - \mathrm{sgn}(nm)\sqrt{|n|}\right)\left[(|n|+1)^{3/2} - \mathrm{sgn}(nm)|n|^{3/2}\right]\eta^2\right\}, \tag{B8}$$

$$a_n^{(2)} = \sqrt{|n|+1}\left(\sqrt{|n|+2} - \mathrm{sgn}(nm)\sqrt{|n|}\right)\eta, \tag{B9}$$

$$a_n^{(3)} = \frac{1}{2}\mathrm{sgn}(m)\sqrt{(|n|+1)(|n|+2)}\left(\sqrt{|n|+3} - \mathrm{sgn}(nm)\sqrt{|n|}\right)^2\eta^2, \tag{B10}$$

and

$$\langle m|\bar{v}_y|n\rangle = \lambda^2 C_{nm}\sum_{j=0}^{3}\left[b_n^{(j)}\delta_{|m|=|n|+j} + b_m^{(j)}\delta_{|n|=|m|+j}\right] + O(\eta^3), \tag{B11}$$

where

$$b_n^{(0)} = -2n\eta, \tag{B12}$$

$$b_n^{(1)} = \mathrm{sgn}(m)\left\{1 - \frac{1}{2}\left(\sqrt{|n|+1} - \mathrm{sgn}(nm)\sqrt{|n|}\right)^3\left[(|n|+1)^{3/2} + \mathrm{sgn}(nm)|n|^{3/2}\right]\eta^2\right\}, \tag{B13}$$

$$b_n^{(2)} = a_n^{(2)}, \quad b_n^{(3)} = a_n^{(3)}. \tag{B14}$$

Appendix C: Calculation of $\langle(\Delta r_l)^2\rangle_N$

In the Landau gauge, which is used in this paper, the x operator is bounded, and calculation of the following matrix elements is straightforward.

$$\langle\Psi_{kN}|\,(x-x_N)^p\,|\Psi_{k'N}\rangle = \frac{\delta_{kk'}\ell^2}{2-\delta_{N0}}\left\{\int_{-\infty}^{\infty}dx h_{|N|}^2(x)x^p \right. \\ \left. -2\,\mathrm{sgn}(n)\eta\int_{-\infty}^{\infty}dx h_{|N|}(x)h_{|N|-1}(x)x^p + (1-\delta_{N0})\int_{-\infty}^{\infty}dx h_{|N|-1}^2(x)x^p\right\} \quad \text{(C1)}$$

where $p=1,2$, and the integrals are calculated as

$$\int_{-\infty}^{\infty}dx h_{|N|}(x)x^p = \frac{\delta_{p2}}{2\lambda}\left(2|N|+1\right), \qquad \int_{-\infty}^{\infty}dx h_{|N|}(x)h_{|N|-1}(x)x^p = \delta_{p1}\sqrt{\frac{|N|}{2\lambda}}, \quad \text{(C2)}$$

which justifies Eqs. (49) and (48). However, the y operator is unbounded, which usually means that the y integral is ill defined and depends on the choice of the limits. We choose the following regularization. We add $\exp\left(-\frac{\epsilon^2}{4}y^2\right)$ where $\epsilon\to 0+$, and, after that, expand the integration limits to infinity:

$$\int_{-\infty}^{\infty}dy\exp\left[i(k-k')y-\frac{\epsilon^2}{4}y^2\right] = 2\pi\frac{\exp\left[-\frac{(k-k')^2}{\epsilon^2}\right]}{\sqrt{\pi}\epsilon}\to 2\pi\delta(k-k'), \quad \text{(C3)}$$

$$\int_{-\infty}^{\infty}dy\exp\left[i(k-k')y-\frac{\epsilon^2}{4}y^2\right]y = -2\pi i\frac{d}{dk}\frac{\exp\left[-\frac{(k-k')^2}{\epsilon^2}\right]}{\sqrt{\pi}\epsilon}\to -2\pi i\delta'(k-k'), \quad \text{(C4)}$$

$$\int_{-\infty}^{\infty}dy\exp\left[i(k-k')y-\frac{\epsilon^2}{4}y^2\right]y^2 = -2\pi\frac{d^2}{dk^2}\frac{\exp\left[-\frac{(k-k')^2}{\epsilon^2}\right]}{\sqrt{\pi}\epsilon}\to -2\pi\delta''(k-k'). \quad \text{(C5)}$$

The matrix elements of the y-operator correspond to the integrals of total derivatives of $h_{|N|}^2(x)$ and $h_{|N|}(x)h_{|N|-1}(x)$, which give zero. The matrix elements of y^2 can be expressed as

$$\left\langle\Psi_{kN}|y^2|\Psi_{k'N}\right\rangle = \frac{\delta_{kk'}\ell^2}{2-\delta_{N0}}\left\{\int_{-\infty}^{\infty}dx\left(h'_{|N|}(x)\right)^2 - \right. \\ \left. 2\,\mathrm{sgn}(n)\eta\int_{-\infty}^{\infty}dx h'_{|N|}(x)h'_{|N|-1}(x) + (1-\delta_{N0})\int_{-\infty}^{\infty}dx\left(h'_{|N|-1}(x)\right)^2\right\}, \quad \text{(C6)}$$

where

$$\int_{-\infty}^{\infty}dx\left(h'_{|N|}(x)\right)^2 = \frac{\lambda}{2}(2|N|+1), \quad \text{and} \quad \int_{-\infty}^{\infty}dx h'_{|N|}(x)h'_{|N|-1}(x) = 0, \quad \text{(C7)}$$

which yields Eq. (50).

---

* iprosk@hosi.phys.s.u-tokyo.ac.jp

[1] H. Fukuyama, Y. Fuseya, M. Ogata, A. Kobayashi, and Y. Suzumura, Physica B: Condensed Matter **407**, 1943 (2012).

[2] K. S. Novoselov, A. K. Geim, S. V. Morozov, D. Jiang, M. I. Katsnelson, I. V. Grigorieva, S. V. Dubonos, and A. A. Firsov, Nature **438**, 197 (2005).

[3] X.-L. Qi and S.-C. Zhang, Rev. Mod. Phys. **83**, 1057 (2011).

[4] N. Tajima, S. Sugawara, M. Tamura, Y. Nishio, and K. Kajita, J. Phys. Soc. Jpn. **75**, 051010 (2006).

[5] S. Katayama, A. Kobayashi, and Y. Suzumura, J. Phys. Soc. Jpn. **75**, 054705 (2006).

[6] H. Kino and T. Miyazaki, J. Phys. Soc. Jpn. **75**, 034704 (2006).

[7] A. Kobayashi, S. Katayama, Y. Suzumura, and H. Fukuyama, J. Phys. Soc. Jpn. **76**, 034711 (2007).

[8] K. Kajita, Y. Nishio, N. Tajima, Y. Suzumura, and A. Kobayashi, J. Phys. Soc. Jpn. **83**, 072002 (2014).

[9] P. Richard, K. Nakayama, T. Sato, M. Neupane, Y.-M. Xu, J. H. Bowen, G. F. Chen, J. L. Luo, N. L. Wang, X. Dai, Z. Fang, H. Ding, and T. Takahashi,

Phys. Rev. Lett. **104**, 137001 (2010).
[10] T. Osada, J. Phys. Soc. Jpn. **77**, 084711 (2008).
[11] T. Morinari and T. Tohyama, J. Phys. Soc. Jpn. **79**, 044708 (2010).
[12] I. A. Luk'yanchuk, A. A. Varlamov, and A. V. Kavokin, Phys. Rev. Lett. **107**, 016601 (2011).
[13] I. Proskurin and M. Ogata, J. Phys. Soc. Jpn. **82**, 063712 (2013).
[14] T. Konoike, M. Sato, K. Uchida, and T. Osada, J. Phys. Soc. Jpn. **82**, 073601 (2013).
[15] N. Tajima, S. Sugawara, R. Kato, Y. Nishio, and K. Kajita, Phys. Rev. Lett. **102**, 176403 (2009).
[16] N. Tajima, M. Sato, S. Sugawara, R. Kato, Y. Nishio, and K. Kajita, Phys. Rev. B **82**, 121420 (2010).
[17] S. Sugawara, M. Tamura, N. Tajima, R. Kato, M. Sato, Y. Nishio, and K. Kajita, J. Phys. Soc. Jpn. **79**, 113704 (2010).
[18] N. Tajima, T. Yamauchi, T. Yamaguchi, M. Suda, Y. Kawasugi, H. M. Yamamoto, R. Kato, Y. Nishio, and K. Kajita, Phys. Rev. B **88**, 075315 (2013).
[19] M. O. Goerbig, J.-N. Fuchs, G. Montambaux, and F. Piéchon, Phys. Rev. B **78**, 045415 (2008).
[20] M. O. Goerbig, J.-N. Fuchs, G. Montambaux, and F. Piéchon, Europhys. Lett. **85**, 57005 (2009).
[21] T. Kawarabayashi, Y. Hatsugai, T. Morimoto, and H. Aoki, Phys. Rev. B **83**, 153414 (2011).
[22] J. Sári, C. Tőke, and M. O. Goerbig, Phys. Rev. B **90**, 155446 (2014).
[23] M. Trescher, B. Sbierski, P. W. Brouwer, and E. J. Bergholtz, Phys. Rev. B **91**, 115135 (2015).
[24] V. Lukose, R. Shankar, and G. Baskaran, Phys. Rev. Lett. **98**, 116802 (2007).
[25] N. H. Shon and T. Ando, J. Phys. Soc. Jpn. **67**, 2421 (1998).
[26] N. M. R. Peres, F. Guinea, and A. H. Castro Neto, Phys. Rev. B **73**, 125411 (2006).
[27] S. G. Sharapov, V. P. Gusynin, and H. Beck, Phys. Rev. B **67**, 144509 (2003).
[28] V. P. Gusynin and S. G. Sharapov, Phys. Rev. B **71**, 125124 (2005).
[29] T. Morinari and T. Tohyama, Phys. Rev. B **82**, 165117 (2010).
[30] Y. Suzumura, I. Proskurin, and M. Ogata, J. Phys. Soc. Jpn. **83**, 023701 (2014).
[31] Y. Suzumura, I. Proskurin, and M. Ogata, J. Phys. Soc. Jpn. **83**, 094705 (2014).
[32] A. Kobayashi, Y. Suzumura, and H. Fukuyama, J. Phys. Soc. Jpn. **77**, 064718 (2008).
[33] M. Monteverde, M. O. Goerbig, P. Auban-Senzier, F. Navarin, H. Henck, C. R. Pasquier, C. Mézière, and P. Batail, Phys. Rev. B **87**, 245110 (2013).
[34] T. Ozawa, T. Yamauchi, N. Tajima, R. Kato, Y. Nishio, and K. Kajita, Meeting abstracts of the Physical Society of Japan **69**, 862 (2014)
[35] T. Morinari, T. Himura, and T. Tohyama, J. Phys. Soc. Jpn. **78**, 023704 (2009).
[36] A. Bastin, C. Lewiner, O. Betbeder-Matibet, and P. Nozieres, J. Phys. Chem. Solids **32**, 1811 (1971).
[37] P. Středa and L. Smrčka, Phys. Status Solidi B **70**, 537 (1975).
[38] S. G. Sharapov, V. P. Gusynin, and H. Beck, Phys. Rev. B **69**, 075104 (2004).
[39] I. S. Gradshteyn and I. M. Ryzhik, *Table of integrals, series, and products*, 7th ed. (Elsevier/Academic Press, Amsterdam, 2007).